A Novel Crowbar Protection Technique for DFIG Wind Farm during Fault Ride Through

Omar Noureldeen[a,b]
[a] Electrical Engineering Department, Faculty of Engineering, Islamic University , Madinah, King Saudi Arabia
[b] Electrical Engineering Department, Faculty of Engineering, South Valley University, Qena, Egypt
E-mail: omar_noureldeen@svu.edu.eg

***Abstract*- This paper proposes a terminal crowbar protection technique for Doubly Fed Induction Generators (DFIG) to protect the rotor converter and enhance network stability during grid disturbances. Simulation test using MATLAB-Simulink toolbox is implemented on a 9 MW wind farm exports its power to 120 KV grid. The simulation is performed using different values of crowbar resistances. The variations of rotor current, rotor speed, DC-link voltage, active power and reactive power of the wind farm are investigated. Also, a comparison between the conventional crowbar and the proposed crowbar protection techniques is investigated.**

Index Terms- DFIG, Conventional Crowbar, Terminal Crowbar, Rotor Current, Active Power, Reactive Power, Short Circuit.

I. INTRODUCTION

Wind energy is one of the fastest growing industries at present and it will continue to grow worldwide, as many countries have plans for future development. The increased penetration of wind energy into power system over the last decade generates new challenges for the power system operators, who have to ensure a reliable and safe grid operation. The use of doubly fed induction machines in modern variable-speed wind turbines has increased rapidly. This development has been driven by the cost reduction as well as the low-loss generation of Insulated Gate Bipolar Transistors (IGBT) [1-3]. According to new grid code requirements, wind turbines must remain connected to the grid during grid disturbances. Moreover, they must also contribute to voltage support during and after grid faults. The crowbar protection system is essential to avoid the disconnection of the doubly fed induction wind generators from the network during faults. The insertion of the crowbar in the rotor circuits for a short period of time enables a more efficient terminal voltage control. As a general rule, the activation and the deactivation of the crowbar system is based only on the DC-link voltage level of the back-to-back converters. However, wind power plants based on the DFIG are very sensitive to grid disturbances, especially to voltage dips. When faults occur and cause voltage dips, subsequently the current flowing through the power converter may be very high over-current. During this situation, it is common to block the converter to avoid any risk of damage, and then to disconnect the generator from the grid [4-7]. Therefore DFIG requires a crowbar protection system disconnects the converter in order to protect it, turning the DFIG generator into a squirrel cage induction generator. The crowbar may comprise of a set of thyristors that will short-circuit the rotor windings when triggered and thereby limit the rotor voltage and provide an additional path for the rotor current. Different values of the crowbar resistances result in a different behavior. Using this technology, the DFIG can stay connected to the grid and resume operation as soon as possible. Several researches have dealt with different crowbar strategies for Low Voltage Ride Through LVRT improvement. The value of crowbar resistance should be chosen carefully. There are two requirements that give an upper and a lower limit to the crowbar resistance. It should be high enough to limit the short circuit rotor current and it should be low enough to avoid too high voltage in the rotor circuit. Also, the optimal crowbar resistance is constrained by the machine rating (MVA rating), rotor current transient and DC-link transient following crowbar deactivation [8-15]. This paper proposes a terminal crowbar resistor connected at the terminal of the DFIG. With the proposed protection techniques, the rotor converter of DFIG is not blocked. Several dynamic simulations are carried out for different terminal crowbar resistance values in case of 150 ms three-phase fault at wind farm terminals. Also, a comparison between the behaviors of DFIG wind farm during three-phase fault with conventional crowbar protection and with proposed crowbar protection is investigated.

II. DFIG SYSTEM MODEL AND CONTROL

The DFIG control and its performance in normal operation have already been discussed in a variety of publications [16-19]. The behavior of DFIG control system during disturbance will be discussed in this section. The DFIG wind turbines utilize a wound rotor induction generator, where the rotor windings are fed through back to back variable frequency, voltage source converter. Figure 1 shows a schematic diagram of the DGIG wind turbines connected grid with conventional crowbar protection. The Rotor Side Converter (RSC) is connected to the Grid Side Converter (GSC) using a DC link. During grid disturbances, due to the magnetic coupling between the stator and the rotor a high rotor current transient is excited. Hence, to avoid damage to the converter, the RSC is short circuited using a resistor bank, which is commonly known as the crowbar protection. The crowbar effectively decouples the back to back converter unit from the wound rotor induction generator, and enables the DFIG to operate as an induction generator [20].

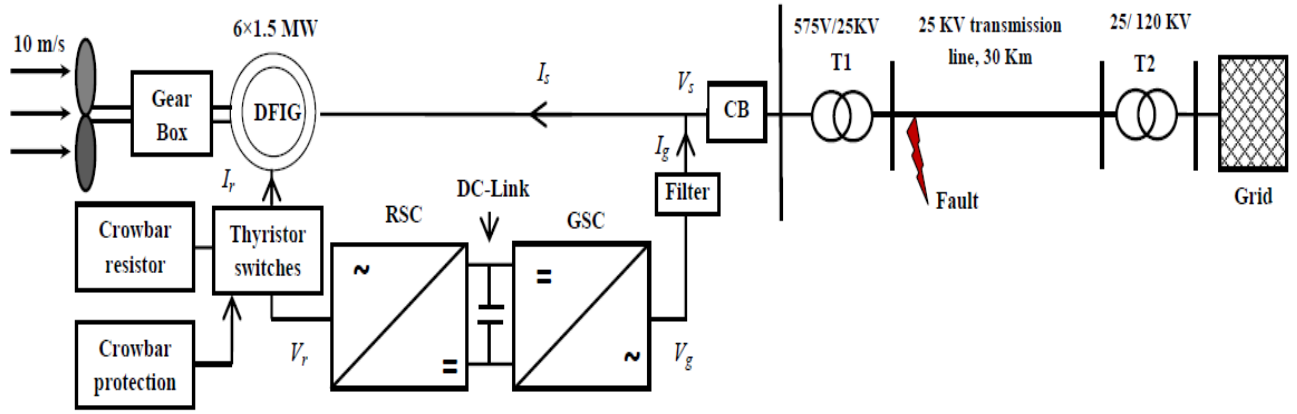

Figure 1 Schematic diagram of the DFIG with conventional crowbar protection

In order to model the DFIG, a standard wound-rotor induction machine component from the SimPowerSystem toolbox has been used. The synchronous *d–q* reference frame has been selected to perform all the simulations [21]:

$$v_{ds} = -R_s i_{ds} - \omega_s \psi_{qs} + \frac{d\psi_{ds}}{dt} \quad (1)$$

$$v_{qs} = -R_s i_{qs} - \omega_s \psi_{ds} + \frac{d\psi_{qs}}{dt} \quad (2)$$

$$v_{dr} = -R_r i_{dr} - \omega_r \psi_{qr} + \frac{d\psi_{dr}}{dt} \quad (3)$$

$$v_{qr} = -R_r i_{qr} - \omega_r \psi_{dr} + \frac{d\psi_{qr}}{dt} \quad (4)$$

where v are voltages (V), i are currents(A), R are resistances (Ω), ψ are flux linkages (V·s). Indices d and q indicate direct and quadrature axis components respectively while s and r indicate stator and rotor quantities respectively. All quantities are referred to the stator.

A. *Rotor Side Converter Control System*

The RSC controls independently the active and reactive power injected by the DFIG into the grid in a stator flux dq-reference frame. Figure 2 shows the control scheme of the RSC. The q-axis current component I_{qr} is used to control the active power using a maximum power tracking strategy to calculate the active power reference [10]. The actual speed of the turbine ω_r is measured and the corresponding mechanical power of the tracking characteristic is used as the reference power for the power control loop. The reference value for the active power P_r is compared with its actual value P and the error is sent to a PI controller which generates the reference value for the *q*-axis current I_{qr_erf}. This signal is compared to its actual value I_{qr} and the error is passed through a second PI controller determining the reference voltage for the *q*-axis component V_{qr}. The *d*-axis is used to control the reactive power exchanged with the grid, which in normal operation is set to zero in order to operate with unity power factor. In case of disturbance, if the induced current in the rotor circuit is not high enough to trigger the over-current protection, the RSC is set to inject reactive power into the grid in order to support the voltage restoration. In such case, the actual voltage V at the collection bus is compared to its reference value V_{ref} and the error is passed through a PI controller to generate the reference signal for the reactive power of the DFIG. Similar to the control strategy of the q component, the error between the reactive power reference and its actual value is passed through a PI controller to determine the reference value for the d-axis current I_{dr_erf}. This signal is compared to the d-axis current value I_{dr} and the error is sent to a third PI controller which determines the reference voltage for the d-axis component V_{dr}.

B. *Grid Side Converter Control System*

The GSC is used to keep DC-link voltage stable under grid fault and fluctuating wind. Figure 3 shows schematic diagram of grid side converter control. In normal operation, the RSC already controls the unity power factor operation and therefore the reference value for the exchanged reactive power between the GSC and the grid is set to zero. In case of disturbance, the GSC is set to inject reactive power into the grid, whether the RSC is blocked or is kept in operation. The control of the GSC is performed using the dq-reference frame. The actual voltage V_{dc} at the DC link is compared with its reference value V_{dc_ref} and the error between both signals is passed through a PI controller which determines the reference signal for the d-axis current $I_{d\_gsc\_ref}$. This latter signal is subtracted with its current value I_{d_gsc} and the error is sent to another PI controller to obtain the reference voltage for the d-axis component. As for the q-axis current, its reference value depends on whether the system operates in normal operation or during disturbance.

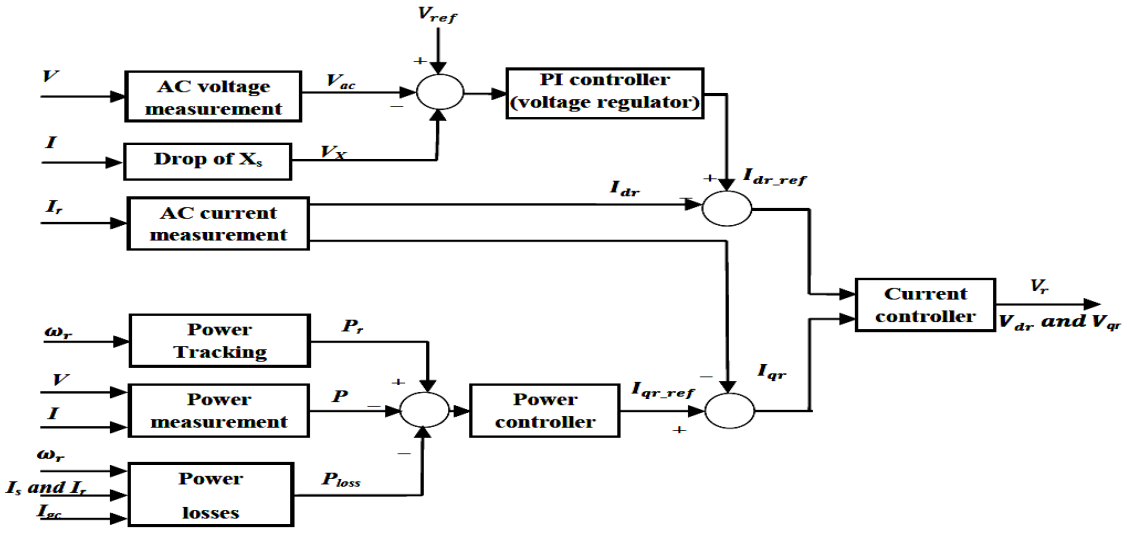

Figure 2 Schematic diagram of rotor side converter control system.

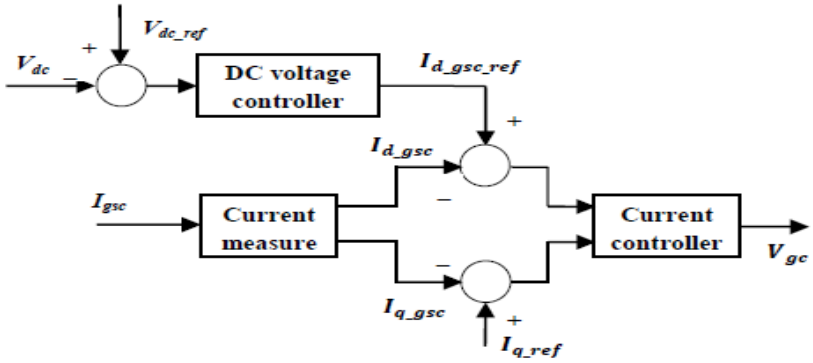

Figure 3 Schematic diagram of grid side converter control system.

In case of disturbance, the actual AC-side voltage of the GSC is compared with its reference value and the error is passed through a PI controller which generates the reference signal for the q-axis current. This reference signal is compared to its current value and the error is sent to a second PI controller which establishes the reference voltage for the q axis component.

III. Dynamic Simulation with Proposed Crowbar Protection

In this section, the dynamic interaction between DFIG wind turbines with power transmission system during and post fault is illustrated and explained. The power system model is similar to the wind farm interconnected grid model with conventional crowbar which it investigated in our paper [20]. The dynamic simulation model is modified by connecting the proposed crowbar protection system at DFIG terminal. As shown in Fig. 4, the dynamic simulation model consists of six 1.5 MW wind turbines connected to a 25-kV distribution system exports power to a 120-kV grid through a 30 km transmission line. The wind turbines operate at 10 m/s wind speed and zero pitch angle, where the maximum turbine output power is 0.55 pu of its rated power. The power characteristics of the wind turbine for different wind speed values are shown in Fig.5. The main data of DFIG wind farm and system parameters are illustrated in Appendix A. The proposed crowbar protection system consists of three resistances in parallel with bidirectional static switches. In normal operations, the static switches remain closed and the DFIG current will not go through crowbar resistances. When the fault is detected by the protection system, the static switches are turned off. In this case, the DFIG current passes through crowbar resistances. The simulation scenario is performed for different value of proposed crowbar resistances as shown in Table 1. The simulated disturbance is a three-phase to ground fault occurs at the wind farm terminals for 150 ms duration, where the protection system detects it after 10 ms from its occurrence. After fault clearance, the crowbar resistance is still connected for 10 ms then it is deactivated. During fault periods, the RSC is not deactivated and still connected to the rotor.

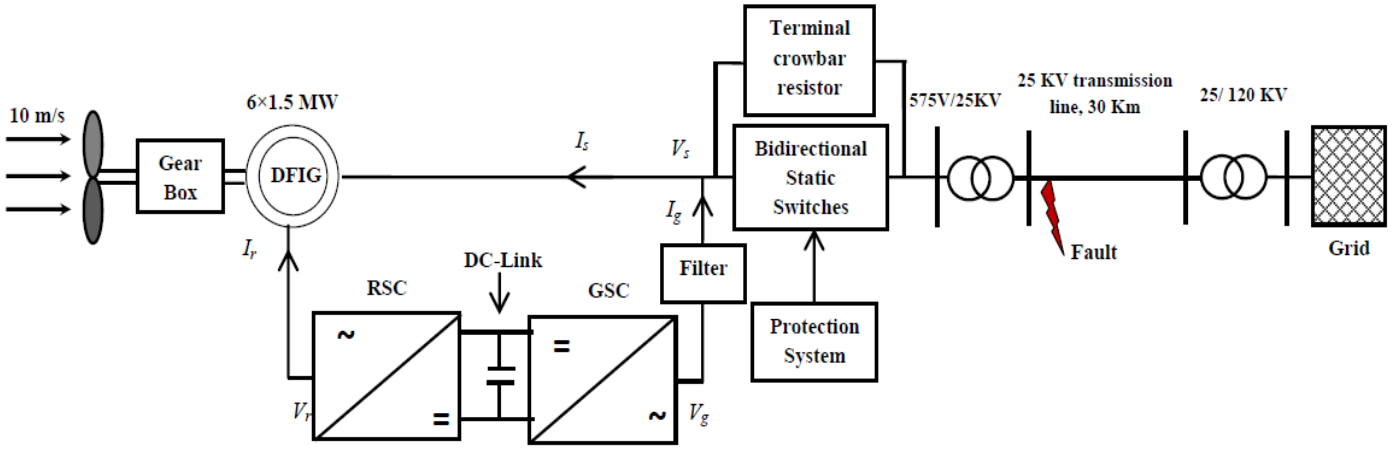

Figure 4 Proposed crowbar protection techniques of DFIG

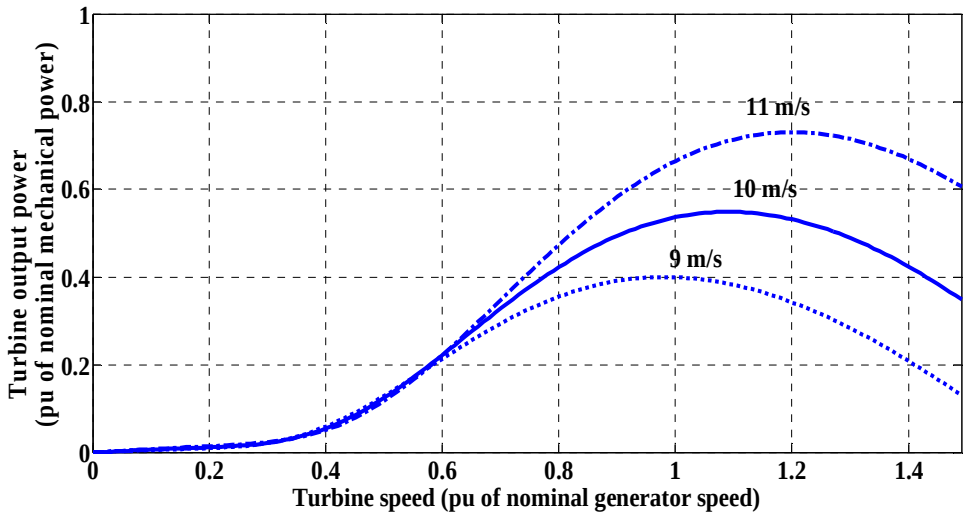

Figure 5 Turbine power characteristic with zero pitch angle.

Table 1: Relations between proposed crowbar resistance (R_terminal) and stator resistance (R_stator).

Case 1	without crowbar resistance
Case 2	R_terminal = 1 × R_stator
Case 3	R_terminal = 5 × R_stator
Case 4	R_terminal = 10 × R_stator
Case 5	R_terminal = 50 × R_stator
Case 6	R_terminal = 100 × R_stator

The wind turbine rotor current, rotor speed, electromagnetic torque, DC-link voltage, active power and reactive power are monitored during grid disturbances. Also, a comparison between the behaviors of DFIG wind turbines with conventional crowbar protection and proposed crowbar protection techniques is investigated.

IV. Simulation Results

The proposed terminal crowbar protection method is verified by SimPowerSystem simulations toolbox. Firstly, the simulation is performed to investigate the effect of different terminal crowbar resistance values to determine the optimal terminal crowbar resistance value. Secondly, investigation of a comparison between the behaviors of DFIG wind turbines in the case of present the optimal value of terminal crowbar resistance and in the case of present the optimal value of conventional crowbar resistance. Where, the optimal value of conventional crowbar resistance equals 10 times of rotor resistance as it is investigated in reference [20].

A. Effect of Terminal Crowbar Resistance Value

Figure 6 shows the variations of the rotor current with the proposed terminal crowbar resistance. During steady state condition, the rotor current value is 0.55 pu while during fault period, the rotor current is increased to 4.35 pu, 3.8 pu and 3 pu for the phases a, b and c respectively when the crowbar resistance is not activated for all studied cases. Figure 6 (a) shows the rotor current variation when the crowbar resistance is not used. It is clear that the rotor current is distorted during

fault period. After fault clearance, the rotor current is increased to 0.99 pu, 1.6 pu and 1.4 pu for the phase a, b and c respectively. As shown in Fig. 6 the rotor current is affected by the value of terminal crowbar resistance during and post fault periods. It is clear that the optimal terminal crowbar resistance value equals 5 times of stator resistance where the current has a little variation during fault period as shown in Fig. 6(c). Also after fault clearance, it has no considerable increase compared with the other cases.

Figure 7 shows the variation of the DFIG rotor speed during fault with different terminal crowbar resistances. In steady state condition the DFIG operates at rotor speed of 1.09 pu. During fault, when the terminal crowbar resistance is not activated, the rotor speed is increased to 1.096 pu and it returns to 1.0942 pu after fault clearing as shown in Fig. 7(a). When the terminal crowbar resistance equals the stator resistance, the rotor speed of DFIG increases to 1.093 pu after fault clearing while it is nearly stable in the case of terminal crowbar resistance equals 5 times of crowbar resistance as shown in Figs. 7 (b),(c). Also after fault clearance, the DFIG rotor speed is increased rapidly when the terminal crowbar resistances are increased to 10, 50 and 100 times of stator resistance as shown in Figs. 7(d), (e) and (f). It is clear that the rotor speed is more stable with proposed terminal crowbar resistance equals 5 times of stator resistance.

Figure 8 shows the variations of the generated active power with different terminal crowbar resistances. Before fault occurrence, the generated active power is 4.95 MW minus the electrical loss in the generator where the wind turbines operate at 10 m/s wind speed and the maximum turbine output power is 0.55 pu of its rated power. As shown in Fig. 8 (a), when the terminal crowbar resistance is not used, the generated active power is decreased to 1.68 MW during fault period and then it is varied between -3.7 MW and 6.6 MW after fault clearance. Then it returns to steady state value. By using terminal crowbar resistance equals stator resistance the generated active power is varied between 2.9 MW and 5.8 MW after fault occurrence while it is varied between -6.3 MW and 6.3 MW after fault clearance as shown in Fig. 8 (b). When the terminal crowbar resistance equals 5 times of stator resistance, the generated active power is varied between 0.97 MW and 7.7 MW after fault occurrence and it is varied between 0.65 MW and 5.4 MW after fault clearance as shown in Fig 8 (c). It is clear that when the terminal crowbar resistance equals 5 times of stator resistance the system returns to steady state condition in short time comparing with the other studied cases. As shown in Fig. 8 (d) the oscillation in the generated power after fault clearance is more than the oscillation in the other cases and it takes long time to be stable. The generated active power is decreased to -1.6 MW after fault occurrence and it returns to 0.7 MW during fault period while it is increased to 10.16 MW after fault clearance where the terminal crowbar resistance equals 50 times of stator resistance as shown in Fig. 8 (e). Also, it increased to 11.48 MW when the terminal crowbar resistance equals 100 times of stator resistance as shown in Fig. 8 (f).

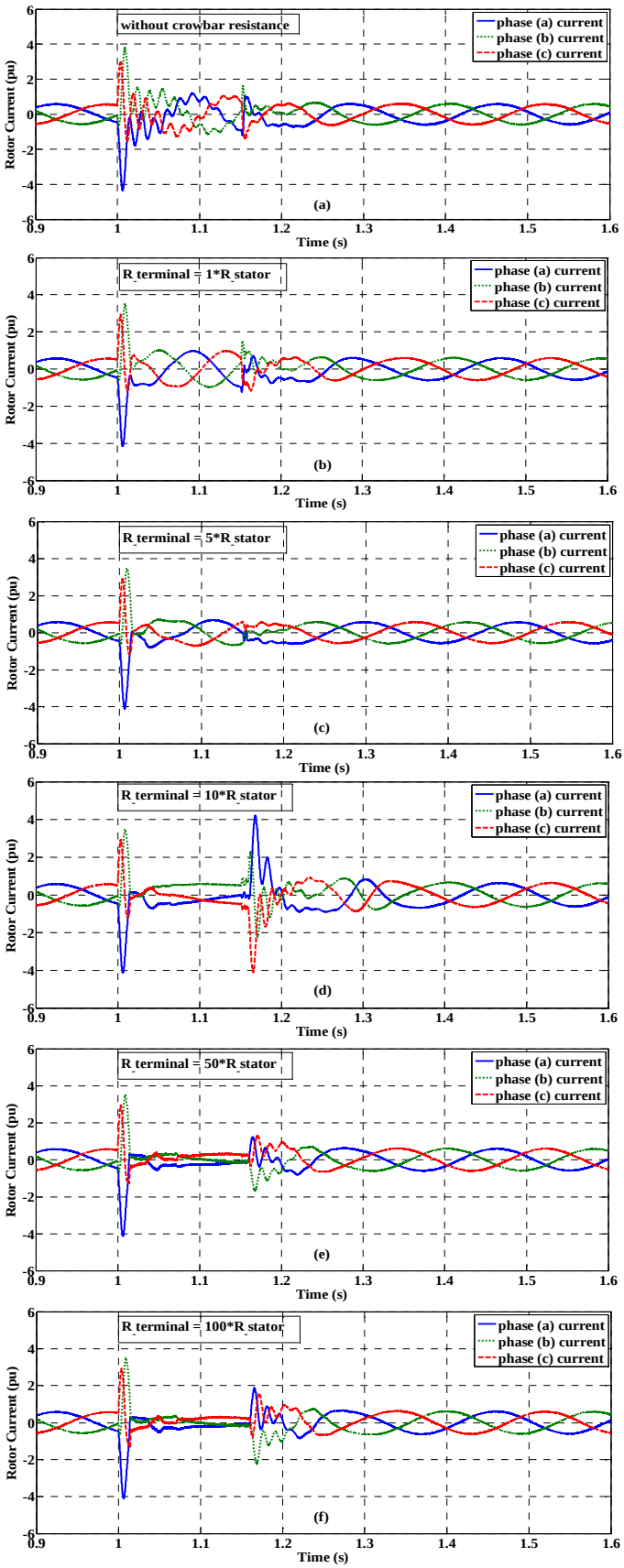

Figure 6 Rotor current variations of DFIG wind farm during fault for different values of the terminal crowbar resistance.

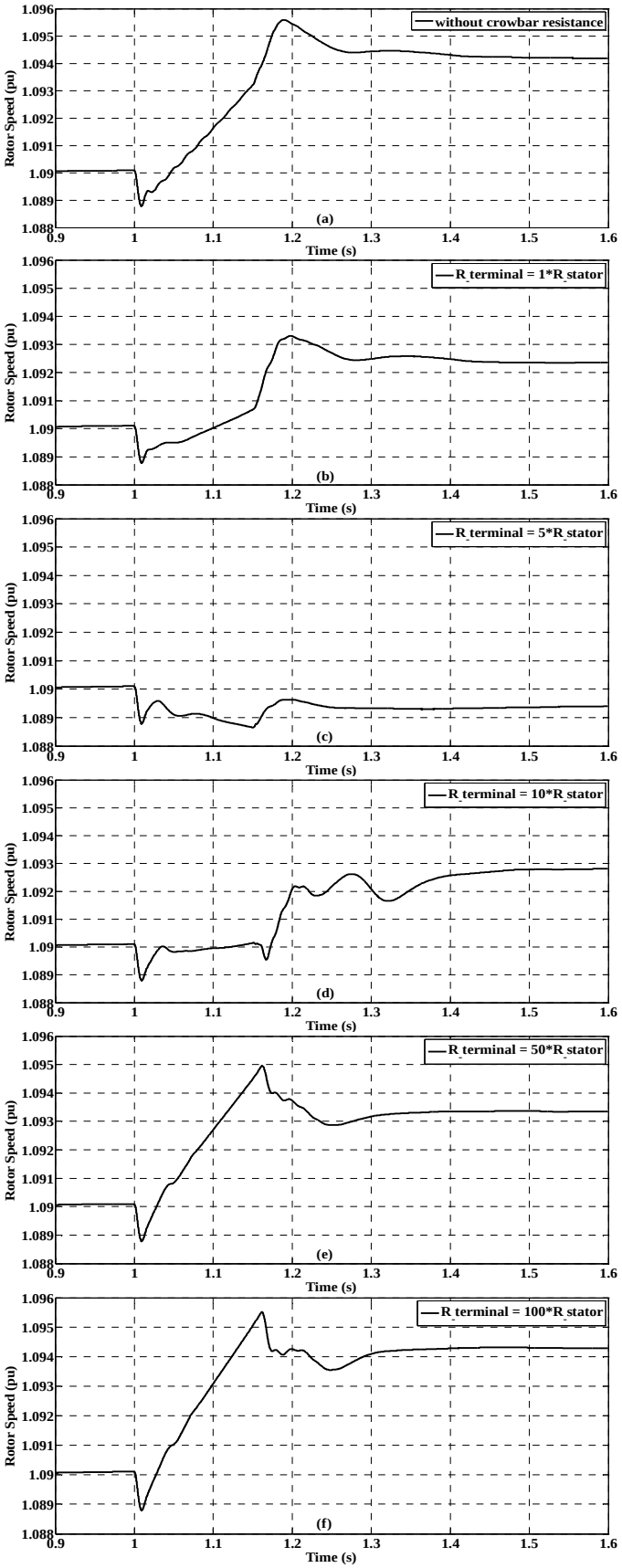

Figure 7 Rotor speed variations of DFIG wind farm during fault for different values of the terminal crowbar resistance.

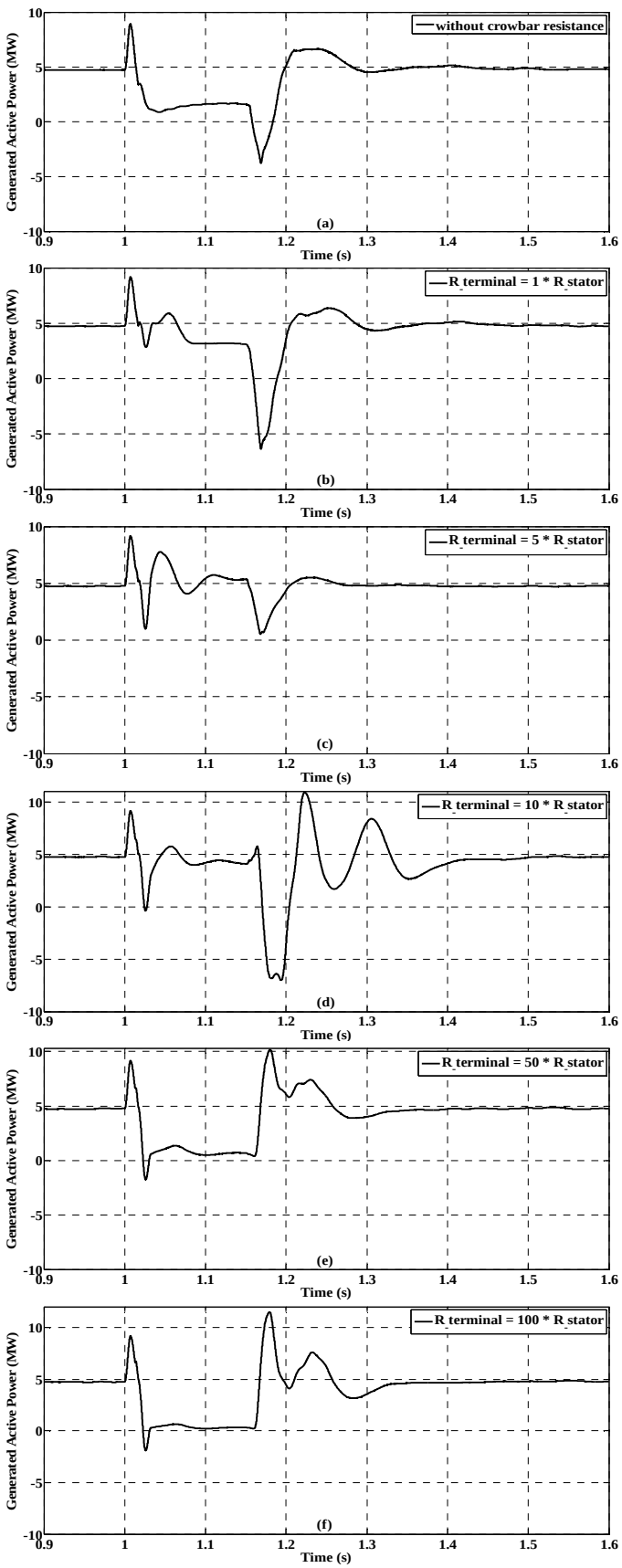

Figure 8 Generated active power variations of DFIG wind farm during fault for different values of the terminal crowbar resistance.

Figure 9 shows the variations of the reactive power with different terminal crowbar resistances during and post fault periods. During steady state condition, the injected or absorbed reactive power by the wind turbine generators is nearly zero. Figure 9 (a) shows that after fault occurrence, in case of crowbar resistance is not activated, the RSC converter acts as Static Synchronous Compensator STATCOM and injects a 6 MVAR reactive power to the grid then it absorbers nearly 1 MVAR reactive power. After fault clearance, the reactive power is fluctuated between 2.9 MVAR and 3.5 MVAR as injected and absorbed reactive power respectively. It is clear that the absorbed or injected reactive power during fault period is decreased by increasing the value of terminal crowbar resistance. Fig. 9 (b) shows after fault clearance in the case of using terminal crowbar resistance equals stator resistance, the variation of reactive power is varied between 4.14 MVAR and 4.7 MVAR as injected and absorbed reactive power respectively. When the terminal crowbar resistance equals 5 times of stator resistance, the reactive power fluctuation is decreased and varied between 1.26 MVAR and 0.87 MVAR after fault clearance as shown in Fig 9 (c). As shown in Fig. 9 (d) the fluctuation of the reactive power is more than the oscillations in the other cases after fault clearance which it is varied between 5.4 MVAR and 8.5 MVAR. As shown in Figs. 9 (e) and (f), the absorbed reactive power is increased by increasing the terminal crowbar resistance after fault clearance. Figure 10 shows the variations of the DC-link voltage during fault with different terminal crowbar resistances. The DC-link capacitance equals 60 mF with nominal voltage of 1200 V. When the system operates without crowbar resistance protection system, the DC-link voltage is increased to 2090 V during fault period. When the terminal crowbar resistance equals rotor resistance, by triggering it at the instant of 1.01 s, the DC-link voltage is increased to 1710 V then it is decreased to 1052 V during fault period as shown in Fig. 10 (b). After fault clearance, the DC-link voltage is varied between 1350 V and 1135 V then it returns to steady state condition. As shown in Fig 10 (c), the DC-link voltage is decreased to 1042 V during fault period and it returns to steady state condition during fault period in the case of terminal crowbar resistance equals 5 times of stator resistance. The system is more unstable with terminal crowbar resistance equals 10 times of stator resistance, where DC-link voltage increases to 2277 V after fault clearance then it decreases to 1081 V as shown in Fig. 10 (d). The fluctuation of the DC-link voltage is increased during and post fault periods when the terminal crowbar resistance increased to 50 and 100 times of stator resistance as shown in Fig. 10 (e) and (f).

Finally, it is clear that the system is more stable when the terminal crowbar resistance equals 5 times of stator resistance. Where the values rotor current, rotor speed, active power, reactive power and DC-link voltage are more stable and low fluctuation during and post fault periods. Also, the system returns to the steady state condition in a time less than that of the other studied cases.

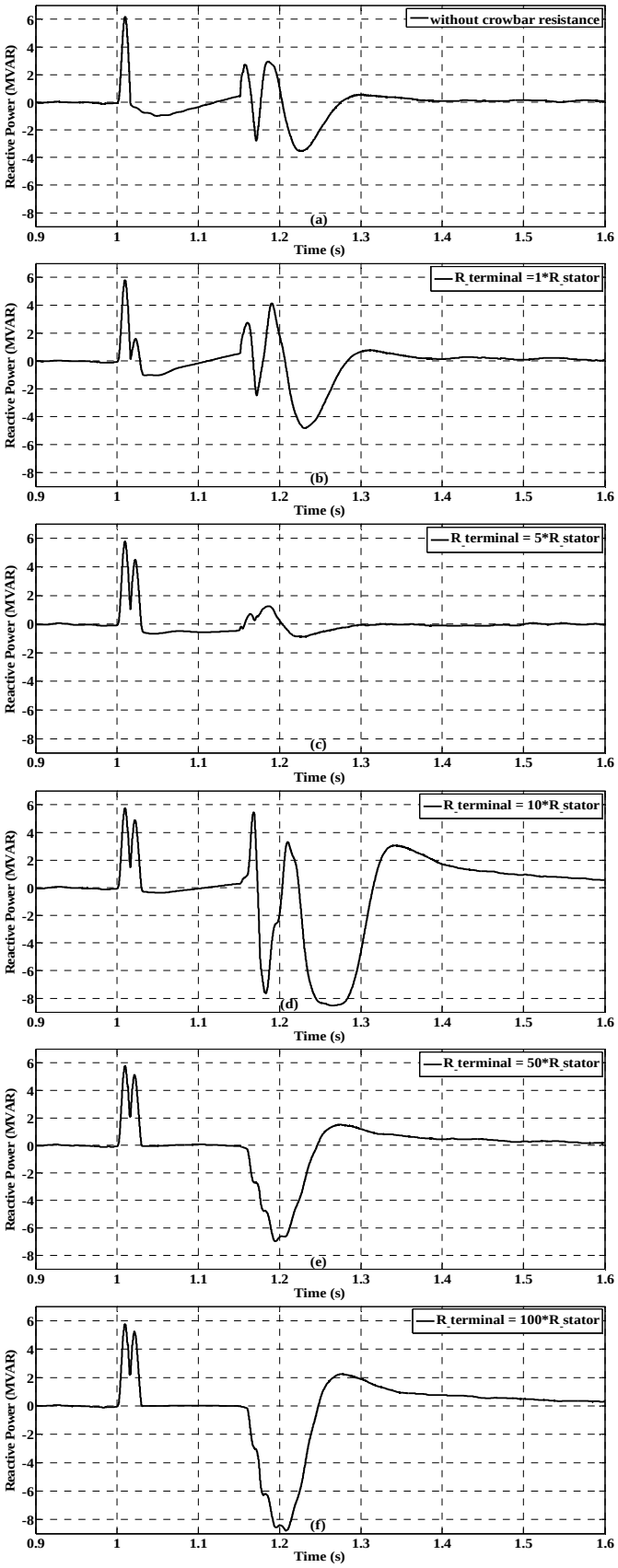

Figure 9 Reactive power variations of DFIG wind farm during fault for different values of the terminal crowbar resistance.

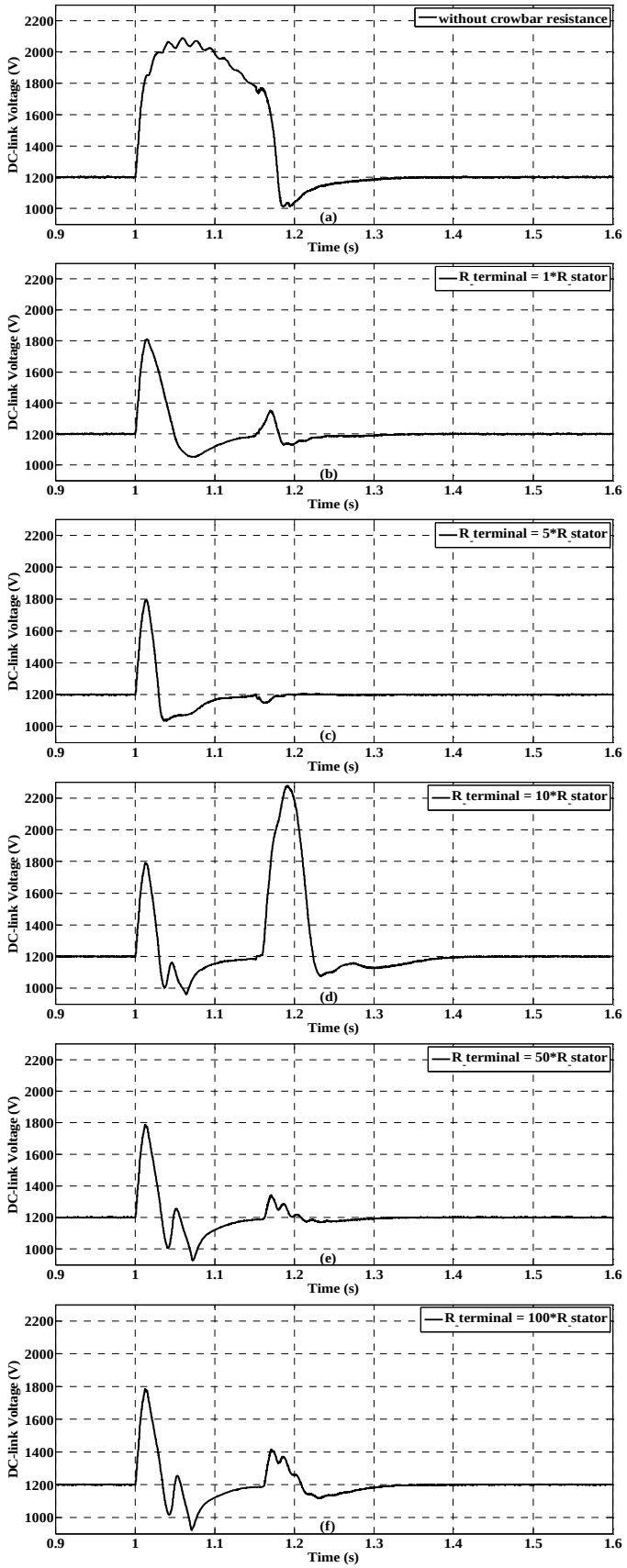

Figure 10 DC-link voltage variations of DFIG wind farm during fault for different values of the terminal crowbar resistance.

B. Comparison Between Conventional and Proposed Crowbar Protection Techniques

In this section, a comparison between the behaviors of the wind turbines generator with conventional crowbar protection and proposed crowbar protection is investigated. This comparison is investigated in the case of present the optimal value of the conventional crowbar resistance and the optimal value of the proposed terminal crowbar resistance protection systems. The optimal value of conventional crowbar resistance equals 10 times of rotor resistance as it is investigated in reference [20]. The optimal value of terminal crowbar protection equals 5 times of stator resistance as it is investigated in the previous section. Figure 11 shows the rotor current variations with different crowbar resistance protection systems. It is clear that the rotor current has a large oscillation with conventional crowbar protection during fault period while it has a little variation with proposed terminal crowbar protection system. Also, the rotor speed with proposed terminal crowbar protection is more stable which it is varied between 1.09 pu and 1.089 pu during and post fault periods while it is varied between 1.09 pu and 1.096 pu with conventional crowbar protection system as shown in Fig. 12.

The variations of the generated active power during and post fault periods are shown in Fig. 13. It is clear that, with terminal crowbar protection system, the wind farm can generate active power during fault period more than the power generated in the present of the conventional crowbar protection system. Figure 14 shows the variations of the reactive power which is injected to the grid or absorbed by the wind turbine generators. It is clear that, after fault clearance, the reactive power fluctuation is varied between 3.5 MVAR and 2.4 MVAR as injected and absorbed reactive power respectively in present of the conventional crowbar protection system. With the proposed terminal crowbar protection system, the reactive power fluctuation is decreased which it is varied between 1.26 MVAR and 0.87 MVAR as injected and absorbed reactive power respectively. Figure 15 shows the variations of the DC-link voltage of the DFIGs during and post fault periods. During fault period, the DC-link voltage is increased to 1736 V and it is decreased to 983 V in present of conventional crowbar protection system. With the proposed terminal crowbar protection system, the DC-link voltage is increased to 1795 V and it is decreased to 1036 V during fault period. It is clear that the DC-link voltage returns to steady state value in a short time with the proposed terminal crowbar protection system comparing with the conventional crowbar protection system. Finally, the operation of DFIG wind turbines in the case of connection the proposed terminal crowbar resistance is stable during fault and it can return to steady state condition in a short time after fault clearance. The fluctuations of rotor current, rotor speed, generated active power, reactive power and DC-link voltage are decreased by using the proposed terminal crowbar protection. Therefore the wind turbine generators can stay connected to the grid during fault and it is not turned off by the protection system.

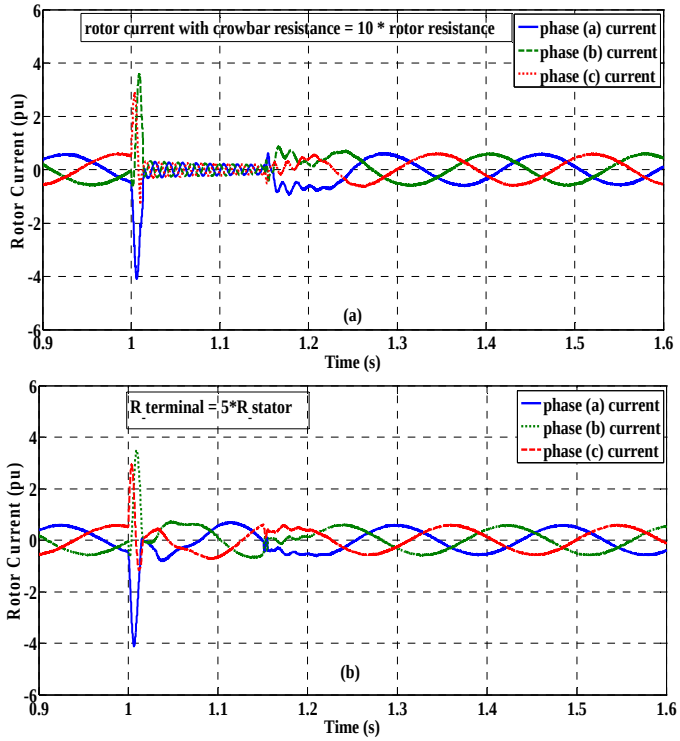

Figure 11 Comparison of rotor current variations during fault for different crowbar protection techniques (a) conventional crowbar protection (b) proposed crowbar protection.

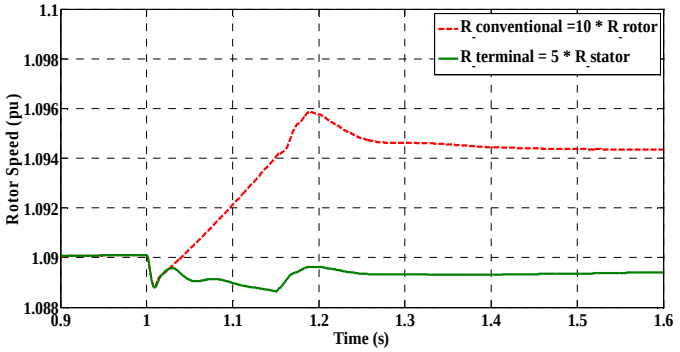

Figure 12 Comparison of rotor speed variations during fault for different crowbar protection techniques.

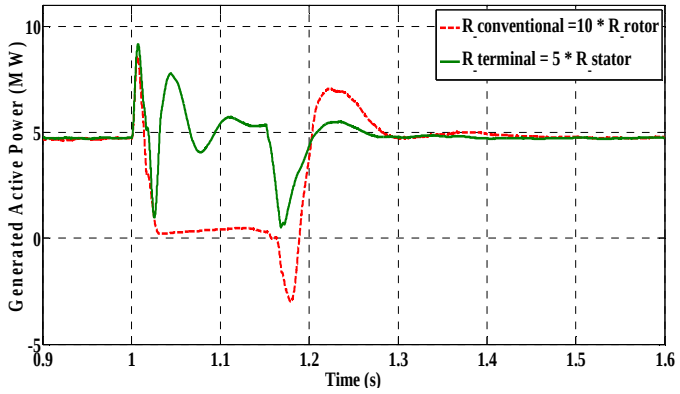

Figure 13 Comparison of active power variations of DFIG wind farm during fault for different crowbar protection techniques.

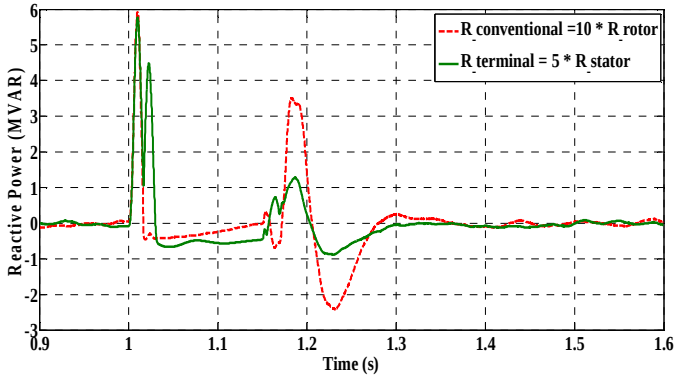

Figure 14 Reactive power variations of DFIG wind farm during fault with different crowbar resistances.

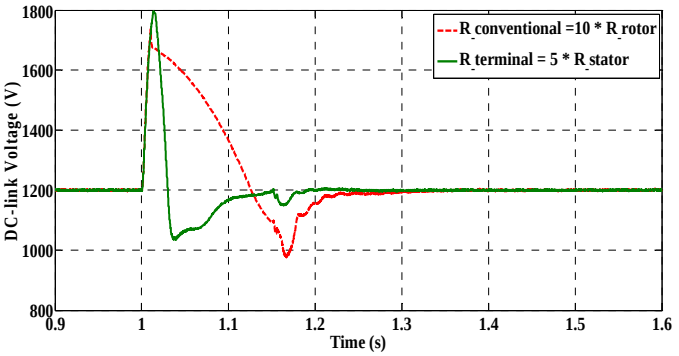

Figure 15 Comparison of DC-link voltage variations during fault for different crowbar protection techniques.

V. CONCLUSIONS

This paper studies the performance of DFIG wind turbine connected grid during three-phase fault in present of proposed terminal crowbar protection system. The proposed terminal crowbar protection system consists of three resistances in parallel with bidirectional static switches which is connected at DFIG terminal. A dynamic model of DFIG wind turbines connected grid is implemented using SimPowerSystem toolbox. The variations of rotor current, rotor speed, generated active power, reactive power and DC-link voltage are investigated during and post fault periods. Several dynamic simulations are carried out for different terminal crowbar resistance values in case of 150 ms three-phase fault occurs at wind farm terminals. The simulation scenario is performed without crowbar protection and with terminal crowbar resistances equal 1, 5, 10, 50 and 100 times of stator resistance. Also, a comparison among the behaviors of DFIG during three-phase fault with proposed terminal crowbar protection and with conventional crowbar protection is investigated. The simulation results show that the system is more stable when the terminal crowbar resistance equals 5 times of stator resistance. In this case, the values of rotor current, rotor speed, active power, reactive power and DC-link voltage have low fluctuations during and post fault periods. Also, the system returns to the steady state condition in a time less than that of the other studied cases.

Also by using the proposed terminal crowbar protection system, the RSC is not deactivated during fault period while it must be deactivated in the case of using the conventional crowbar protection techniques. Through this study, we recommend that, the impacts of different fault types and different fault duration times on the stability of system must be studied.

APPENDIX A. DFIG DATA AND SYSTEM PARAMETERS

DFIG parameters	
Rated power (MW)	1.5
Rated voltage (V)	575
Rated frequency (Hz)	60
Stator resistance (pu)	0.004843
Rotor resistance (pu)	0.004377
Stator leakage inductance (pu)	0.1248
Rotor leakage inductance (pu)	0.1791
Mutual inductance (pu)	6.77
Transmission line parameters	
Positive sequence resistance (ohm/km)	0.1153
Zero sequence resistance (ohm/km)	0.413
Positive sequence inductance (henries/km)	0.00105
Zero sequence inductance (henries/km)	0.00332
Positive sequence capacitance (farads/km)	11.33e-9
Zero sequence capacitance (farads/km)	5.01e-9
Transformer(T1) parameter	
Rated power (MVA)	12
Turns ratio	575V/25KV
Impedance (pu)	0.0017+j0.05
Transformer(T2) parameter	
Rated power (MVA)	47
Turns ratio	25KV/120KV
Impedance (pu)	0.00534+j0.16
Grid impedance	
Impedance (pu)	0.0004+j0.004

REFERENCES

[1] Omar Noureldeen, Mahmoud Rihan, Barakat Hasanin, "Stability improvement of fixed speed induction generator wind farm using STATCOM during different fault locations and durations", ScienceDirect, Ain Shams Engineering Journal (2011) 2, 1–10, doi:10.1016/j.asej.2011.04.002.

[2] S. Sajedi, F. Khaliefah, T. Karimi, Z. Khaliefah, "Fault ride through protection of DFIG based wind generation system", Research Journal of Applied Sciences, Engineering and Technology, 4 (5), (2012), pp. 428-432.

[3] Min Min Kyaw, V.K. Ramachandaramurthy, "Fault ride through and voltage regulation for grid connected wind turbine", ScienceDirect, Renewable Energy 36 (2011) 206-215, doi:10.1016/j.renene.2010.06.022.

[4] Xueqin Zheng, Donghui Guo, "A Noval Ride-through control strategy of DFIG wind generation under grid voltage dip, Journal of Information & computational Science, 8 (3), (2011), pp. 579-591.

[5] M. Rahimi, M. Parniani, "Grid fault ride through analysis and control of wind turbines with doubly fed induction generators", Science direct, Electrical Power System Research, 80, 2010, pp. 184-195.

[6] M. Rahimi, M. Parniani, "Efficient control of wind turbines with doubly fed induction generators for low-voltage ride-through capability enhancement", IET Renewable Power Generation, 4 (3), 2010, pp. 242-252, doi: 10.1049/iet-rpg.2009.0072.

[7] Anca D. Hansen, Gabriele Michalke, "Fault ride-through capability of DFIG wind turbines" ScienceDirect, Renewable Energy 32 (2007) 1594–1610, doi:10.1016/j.renene.2006.10.008.

[8] Jin Yang, John E. Fletcher, O' Reilly, "A series-dynamic-resistor-based converter protection scheme for doubly-fed induction generator during various fault conditions" IEEE Transactions on Energy Conversion, 25 (2) June 2010.

[9] Francois B., Yongdong Li , "Improved Crowbar Control Strategy of DFIG Based Wind Turbines for Grid Fault Ride-Through" Applied Power Electronics Conference and Exposition, 2009, pp. 1932 - 1938 , doi. 10.1109/APEC.2009.4802937.

[10] S. Chondrogiannis, M. Barnes, "Specification of rotor side voltage source inverter of a doubly-fed induction generator for achieving ride-through capability", IET Renewable Power Generation, vol. 2, no. 3, 2008, pp. 139–150.

[11] Mingyu Wang, Bin Zhao, Hui Li, Chao Yang, Renjie Ye, Z. Chen, "Investigation of Transient Models and Performances for a Doubly Fed Wind Turbine under a Grid Fault" WSEAS TRANSACTIONS on CIRCUITS and SYSTEMS 11 (10), November 2011.

[12] L. Shi, N. Chen and Q. Lu, "Dynamic Characteristic Analysis of Doubly-fed Induction Generator Low Voltage Ride-through", ScienceDirect, Energy Procedia 16 (2012) 1526 – 1534, doi:10.1016/j.egypro.2012.01.239.

[13] Christian Wessels, Fabian Gebhardt and Friedrich W. Fuchs, "Dynamic Voltage Restorer to allow LVRT for a DFIG Wind Turbine", IEEE International Symposium on Industrial Electronics (ISIE), 2010, doi: 10.1109/ISIE.2010.5637336.

[14] J. Lopez, P. Sanchis, X. Roboam, L. Marroyo "Dynamic behavior of doubly fed induction generator during three phase voltage dips" IEEE Transactions on Energy Conversion, vol. 22, no. 3, 2007, pp. 709-717..

[15] M. Garcia-Gracia, M. P. Comech, J. Sallan, and A. Llombart, "Modelling wind farms for grid disturbance studies", Science direct, renewable energy, 33, 2008, pp. 2109-2121.

[16] Kasem AH, El-Saadany EF, El-Tamaly HH, Wahab, MAA, "An improved fault ride through strategy for doubly fed induction generator-based wind turbines IET Renewable Power Generation 2 (4), 2008, pp. 201-214.

[17] Hansen AD, Jauch C, Sorensen P, Iov F, Blaabjerg F. "Dynamic wind turbine models in power system" simulation tool DIgSILENT, Riso-R-1400(EN), 2003.

[18] Leonhard W., "Control of electrical drives" , Berlin, Springer, 2001.

[19] Pena R, Clare JC, Asher GM., "Doubly-fed induction generator using back-to-back PWM converters and its application to variable speed wind-energy generation", IEE Proc Electron. Power Appl., 143(3), 1996;:231–241.

[20] Omar Noureldeen, "Behavior of DFIG Wind Turbines with Crowbar Protection under Short Circuit ", International Journal of Engineering & Science 12 (3), 2012, pp. 32-37.

[21] "MATLAB/Simulink Documentation". Available: http://www.mathworks.com.

Omar Noureldeen is an assistant professor in the department of electrical engineering, Faculty of Engineering ,Qena, South Valley University, Egypt. He received his Ph. D. in electrical power and machines from Faculty of Engineering, Cairo University in 2004. From 2004 to 2006 he has been assistant professor at the department of electrical engineering, Higher Institute of Energy, South Valley University. Since 2007 he is assistant professor at the department of electrical engineering, Faculty of Engineering - Qena, South Valley University. Since 2011 till now he is assiatant professor at the department of electrical engineering, Faculty of Engineering, Islamic University, Madinah, King Saudi Arabia. His fields of interest are digital protection of power systems, power system stability, and renewable energy systems.